Rottmann, M., Schröder, H. C., Gramzow, M., Renneisen, K., Kurelec, B., Dorn, A., Friese, U., & Müller, W. E. G. (1987) *EMBO J. 6*, 3939-3944.
Sahyoun, N., Wolf, M., Besterman, J., Hsieh, T., Sander, M., LeVine, H., III, Chang, K.-J., & Cuatrecasas, P. (1986) *Proc. Natl. Acad. Sci. U.S.A. 83*, 1603-1607.
Sander, M., & Hsieh, T. (1983) *J. Biol. Chem. 258*, 8421-8428.
Sander, M., Nolan, J. M., & Hsieh, T. (1984) *Proc. Natl. Acad. Sci. U.S.A. 81*, 6938-6942.
Schomburg, U., & Grosse, F. (1986) *Eur. J. Biochem. 160*, 451-457.
Shelton, E. R., Osheroff, N., & Brutlag, D. L. (1983) *J. Biol. Chem. 258*, 9530-9535.
Sullivan, D. M., Glisson, B. S., Hodges, P. K., Smallwood-Kentro, S., & Ross, W. E. (1986) *Biochemistry 25*, 2248-2256.
Taudou, G., Mirambeau, G., Lavenot, C., der Garabedian, A., Vermeersch, J., & Duguet, M. (1984) *FEBS Lett. 176*, 431-435.
Vosberg, H.-P. (1985) *Curr. Top. Microbiol. Immunol. 114*, 19-102.
Wang, J. C. (1985) *Annu. Rev. Biochem. 54*, 665-697.
Yanagida, M., & Wang, J. C. (1987) *Nucleic Acids and Molecular Biology* (Eckstein, F., & Lilly, D. M. J., Eds.) Vol. 1, pp 196-209, Springer-Verlag, Berlin.
Zwelling, L. A., Estey, E., Silberman, L., Doyle, S., & Hittelman, W. (1987) *Cancer Res. 47*, 251-257.

# Thermotropic Properties of Saturated Mixed Acyl Phosphatidylethanolamines†

Jeffrey T. Mason*,‡ and Frances A. Stephenson§

*Department of Cellular Pathology, The Armed Forces Institute of Pathology, Washington, D.C. 20306-6000, and Department of Biochemistry, The University of Virginia School of Medicine, Charlottesville, Virginia 22908*

*Received May 23, 1989; Revised Manuscript Received September 5, 1989*

ABSTRACT: The mixed acyl phosphatidylethanolamine (PE) series C(18)C(18)PE, C(18)C(16)PE, C(18)C(14)PE, C(18)C(12)PE, and C(18)C(10)PE has been prepared from the corresponding phosphatidylcholines by phospholipase D mediated transphosphatidylation. The thermotropic behavior of unhydrated and hydrated preparations of these PEs has been investigated by differential scanning calorimetry and $^{31}P$ NMR spectroscopy. Unhydrated preparations of the PEs undergo crystalline to liquid-crystalline transitions ($T_{m+h}$), which correspond to the simultaneous hydration and acyl chain melting of poorly hydrated crystalline samples. Hydrated preparations of the PEs undergo gel to liquid-crystalline transitions ($T_m$) when scanned immediately subsequent to cooling from temperatures above their respective $T_{m+h}$s. Multilamellar bilayers of C(18)C(18)PE, C(18)C(16)PE, and C(18)C(14)PE pack without significant interdigitation of the phospholipid acyl chains across the bilayer center in the gel phase. C(18)C(10)PE multilamellar preparations exhibit a mixed-interdigitated gel phase packing of the phospholipid acyl chains. Hydrated bilayers of C(18)C(12)PE adopt a mixed-interdigitated gel phase packing at temperatures below 13.9 °C. Between 13.9 °C and the gel to liquid-crystalline transition temperature of 36.9 °C, the C(18)C(12)PE bilayer adopts a noninterdigitated gel phase packing. The metastable behavior of fully hydrated and partially hydrated preparations of the mixed acyl PEs has been investigated. Bilayers of C(18)C(18)PE, C(18)C(16)PE, and C(18)C(14)PE exhibited little or no tendency toward regeneration of the crystalline phase. In contrast, bilayers of C(18)C(12)PE and C(18)C(10)PE exhibited a metastability of the liquid-crystalline phase in the temperature interval between $T_m$ and $T_{m+h}$, which can allow for the regeneration of the crystalline phase under certain conditions. Bilayers of C(18)C(12)PE exhibited an additional metastability of the noninterdigitated gel phase.

Phosphatidylethanolamines (PEs)[1] represent the second largest phospholipid component of mammalian plasma membranes after the PCs (Rouser et al., 1986). In addition, PE has been shown to be the major membrane phospholipid in many prokaryotes (Overath & Thilo, 1978). For these reasons, the membrane properties of naturally occurring and synthetic PEs are a topic of considerable interest in membrane research.

Until a few years ago, it was thought that the thermotropic properties of saturated chain PEs were simpler than those of their PC counterparts However, recent studies have revealed a complex polymorphism for these PEs. When saturated symmetric chain PEs with chain lengths from C(11) to C(20) are suspended in buffer at room temperature, a crystalline subphase ($L_c$) results. When these phases are heated, crystalline to liquid-crystalline ($L_c \rightarrow L_\alpha$) phase transitions are observed. These transitions are assigned to the simultaneous

† This work was supported in part by Grant GM-33040 from the National Institutes of Health and by a grant from The American Registry of Pathology.

* Correspondence should be addressed to this author.
‡ The Armed Forces Institute of Pathology.
§ The University of Virginia, School of Medicine.

[1] Abbreviations: PC, phosphatidylcholine; PE, phosphatidylethanolamine; C($x$)C($y$)PC(PE), a saturated acyl phosphatidylcholine (phosphatidylethanolamine) with $x$ carbons in the *sn*-1 acyl chain and $y$ carbons in the *sn*-2 acyl chain; DSC, differential scanning calorimetry; TLC, thin-layer chromatography; Tris, tris(hydroxymethyl)aminomethane; CSA, chemical shift anisotropy; $T_m$, gel to liquid-crystalline transition temperature; $T_{m+h}$, crystalline to liquid-crystalline transition temperature; $L_\beta$, gel bilayer phase (untilted chains); $L_c$, crystalline bilayer phase; $L_\alpha$, liquid-crystalline bilayer phase.

0006-2960/90/0429-590$02.50/0 

hydration and acyl chain melting of a poorly hydrated crystalline sample (Mantsch et al., 1983; Chang & Epand, 1983; Xu et al., 1988). When samples that have been heated through the crystalline to liquid-crystalline transition are cooled and immediately rescanned, reversible gel to liquid-crystalline ($L_\beta \leftrightarrow L_\alpha$) phase transitions are observed. The gel to liquid-crystalline transitions ($T_m$) occur at a lower temperature than the crystalline to liquid-crystalline transitions ($T_{m+h}$). However, the difference in the two transition temperatures decreases with increasing chain length and extrapolates to a value of zero at a chain length of C(20) (Chowdhry et al., 1984). Recently, both the gel ($L_\beta$) and liquid-crystalline ($L_\alpha$) phases of fully hydrated symmetric chain PEs have been shown to exhibit metastable behavior. Incubation of the metastable $L_\beta$ phase of C(12)C(12)PE (Chang & Epand, 1983) and C(14)C(14)PE (Wilkinson & Nagle, 1984) at supercooling temperatures results in the regeneration of the $L_c$ phase under certain experimental conditions. Supercooling of the gel phase can also lead to the formation of stable intermediates other than the $L_c$ crystalline phase. When heated, these stable intermediates can undergo transitions to the gel phase at temperatures below $T_m$ in hydrated bilayers of C(14)C(14)PE and C(16)C(16)PE (Mulukutla & Shipley, 1984) or can transform directly to the liquid-crystalline phase at temperatures between $T_m$ and $T_{m+h}$ in bilayers of C(12)C(12)PE (Seddon et al., 1983). These stable intermediates are highly ordered and appear to differ from the $L_c$ crystalline phase in the strength of their lateral chain interactions, the tilt of the hydrocarbon chains to the bilayer normal, and the degree of headgroup hydration (Seddon et al., 1983, 1984). Within the temperature interval between $T_m$ and $T_{m+h}$ ($\Delta T$ region), the liquid-crystalline phase is metastable with respect to the $L_c$ phase of some hydrated PE bilayers. Incubation of the $L_\alpha$ phase of C(11)C(11)PE (Xu et al., 1988), C(12)C(12)PE (Seddon et al., 1983), or C(14)C(14)PE (Wilkinson & Nagle, 1984) within the $\Delta T$ region can result in the direct conversion to the $L_c$ crystalline phase under certain experimental conditions. In general, the metastable phase behavior of the symmetric chain PEs decreases with increasing chain length (Seddon et al., 1984).

In this investigation, we extend the studies on saturated PEs by reporting on the bilayer properties of the saturated mixed chain PE series C(18)C(16)PE, C(18)C(14)PE, C(18)C(12)PE, and C(18)C(10)PE as revealed by high-sensitivity DSC and $^{31}P$ NMR spectroscopy. The interpretation of these results will be aided by our previous work on the corresponding mixed chain PC series (Mason et al., 1981b; Hui et al., 1984; Huang & Mason, 1986).

## Materials and Methods

*Synthesis and Purification of Phospholipids.* Synthetic C(18)C(18)PC (lot C180-45) was purchased from Avanti Polar Lipids, Inc., Birmingham, AL. The mixed acyl PCs C(18)C(16)PC, C(18)C(14)PC, C(18)C(12)PC, and C(18)C(10)PC were synthesized and purified by established procedures (Mason et al., 1981a). The mixed acyl PCs were ≥98 mol % isomerically pure with regard to the positional specificity of the acyl chains on the glycerol backbone. The above PCs were converted to the corresponding PEs by a modification of the method of Comfurius and Zwaal (1977). This modification entailed the colyophilization of the saturated PC substrate with an equimolar amount of sodium dodecyl sulfate. The phospholipase D mediated transphosphatidylation of the higher molecular weight PCs would not proceed to completion unless sodium dodecyl sulfate was included as a promoter.

The PEs were purified by silicic acid chromatography (Biosil A, 100–200 mesh, Bio-Rad) employing a low-pressure chromatography system. The PEs were eluted with an isochratic solvent system of chloroform/methanol/water (65:25:4). All of the PEs were precipitated twice from acetone/chloroform (95:5), dried under vacuum over $CaSO_2$, and finally stored as dry powders under nitrogen at −20 °C until used. The PEs were analyzed by TLC on 250-μm silica gel G plates by using a solvent system of chloroform/methanol/48% ammonium hydroxide (65:35:5) and then were visualized with iodine. In all cases, only a single spot, corresponding to authentic PE, was observed at a loading of about 1 μmol of lipid.

*Preparation of Samples for DSC and NMR.* After lyophilization from benzene/methanol (95:5), the PEs were dispersed in 50 mM KCl, 5 mM EDTA, and 10 mM Tris buffer at pH 8.1. For DSC measurements, a concentration of 10 mg/mL was employed. For $^{31}P$ NMR experiments, a concentration of 100 mg/mL was used, and $D_2O$ [5% (v/v)] was added to the preparation to serve as an internal field/frequency lock. Samples for $^{31}P$ NMR measurements were prepared in 10-mm (i.d.) NMR tubes. The PE solutions were thoroughly mixed and allowed to incubate at 80 °C for 24 h. The samples were then rapidly frozen by brief incubation in a cold bath (−60 °C) and were allowed to slowly thaw at 2 °C. After an additional freeze/thaw cycle, the samples were subjected to a final incubation at 80 °C for 24 h. This extensive incubation protocol was necessary to ensure complete hydration of the PEs. Unhydrated PE samples were also prepared such that the suspended samples were not heated above 2 °C. For these preparations, the lyophilized PEs and buffer, both at 0 °C, were thoroughly mixed on a Vortex mixer. The samples were then rapidly frozen in a cold bath (−60 °C) and were allowed to slowly thaw at 2 °C. After an additional freeze/thaw cycle, the PE suspensions were immediately used for DSC or $^{31}P$ NMR measurements. The term "unhydrated" in this context is taken to mean a sample that has not been heated above its $T_{m+h}$ in the presence of water. In the case of saturated symmetric chain PEs, this results in a poorly hydrated crystalline PE preparation (Chang & Epand, 1983). In the case of DSC measurements, weighed amounts of buffer and dry lipid were added to calorimeter vials, which were then sealed. The unhydrated PE samples were then processed directly in the calorimeter vials.

*$^{13}P$ NMR Spectroscopy.* All phosphorus NMR spectra of the PE preparations were obtained at 24.15 MHz using quadrature detection with a JOEL-FX60Q (Peabody, MA) Fourier-transform spectrometer operating under continuous broad-band proton noise decoupling at at power of 5 W, as described previously (Huang et al., 1986). A 4000-Hz sweepwidth was employed, and 4000 data points were collected with 5000–20000 scans accumulated per spectrum at a delay of 1 s between pulses. A line broadening of 10 Hz was introduced during signal enhancement for the broad asymmetric line shapes.

*DSC.* All DSC runs were performed on a Hart 7707 series differential scanning microcalorimeter (Hart Scientific, Provo, UT) equipped for microcomputer control of data acquisition and analysis. The Hart microcalorimeter is of the heat conduction type and was calibrated by a procedure recommended by the manufacturer. Samples to be analyzed (~500 μL of solution) were loaded into 1-mL stainless-steel vials, which were sealed and incubated in the calorimeter at the desired starting temperature. The solutions were allowed to come to thermal equilibrium, which typically required 1 h, prior to the initiation of the run. Scans were performed in both ascending

Table I: Thermodynamic Parameters of the Mixed Acyl Phosphatidylethanolamines[a]

| phospholipid | unhydrated | | | hydrated (ascending scans) | | | hydrated (descending scans) | | |
|---|---|---|---|---|---|---|---|---|---|
| | $T_m$ | $\Delta T_{1/2}$ | $\Delta H$ | $T_m$ | $\Delta T_{1/2}$ | $\Delta H$ | $T_m$ | $\Delta T_{1/2}$ | $\Delta H$ |
| C(18)C(18)PE | 74.2 | 0.51 | 22.2 | 72.9 | 1.2 | 10.9 | 71.0, 71.9 | 1.2 | 11.1 |
| C(18)C(16)PE | 65.8 | 0.81 | 14.6 | 64.4 | 1.9 | 9.2 | 62.6, 63.6 | 1.4 | 8.8 |
| C(18)C(14)PE | 58–62 | 3.1 | 13.2 | 53.5 | 2.2 | 6.8 | 52.4 | 1.0 | 7.0 |
| C(18)C(12)PE[b] | 50.8 | 1.0 | 14.2 | 13.9 | 1.4 | 2.6 | 12.4 | 1.1 | 2.5 |
| C(18)C(12)PE[c] | | | | 36.9 | 2.3 | 4.2 | 35.3 | 1.7 | 4.1 |
| C(18)C(10)PE | 39.2 | 1.2 | 12.2 | 21.1 | 1.0 | 9.2 | 17.9, 20.1 | 0.64, 0.54 | 9.8 |

[a] Thermodynamic parameters of the mixed acyl PEs in excess buffer at a concentration of 10 mg/mL. All scans were at 10 °C/h except the descending scan of the hydrated C(18)C(12)PE sample, which was at 60 °C/h. Values of $\Delta T_{1/2}$ and $T_m$ are in degrees centigrade, and values of $\Delta H$ are in kilocalories per mole. [b] Values for the low-temperature transition of hydrated C(18)C(12)PE. [c] Values for the high-temperature transition of hydrated C(18)C(12)PE.

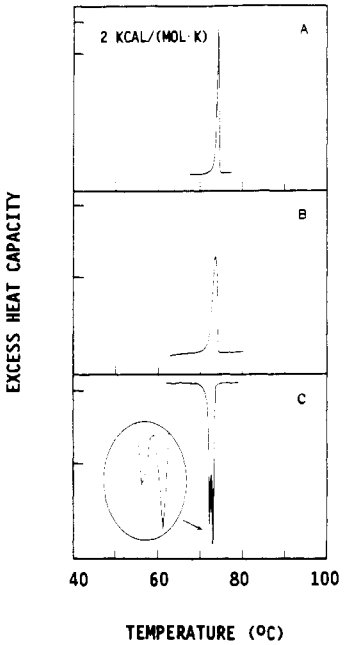


FIGURE 1: DSC profiles of C(18)C(18)PE in excess buffer. (A) Ascending scan of an unhydrated preparation. (B) Ascending scan of a hydrated preparation. (C) Descending scan of a hydrated preparation. The inset in panel C reveals the fine structure of the exotherm seen in the descending scan of the hydrated preparation. Phospholipid concentrations were 10 mg/mL, and scan rates were 10 °C/h. Details of sample preparation are given in the text.

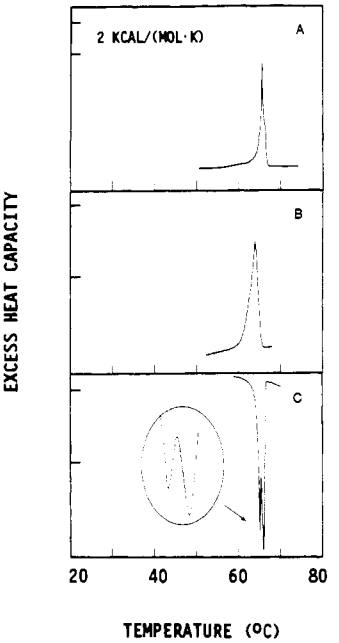


FIGURE 2: DSC profiles of C(18)C(16)PE in excess buffer. (A) Ascending scan of an unhydrated preparation. (B) Ascending scan of a hydrated preparation. (C) Descending scan of a hydrated preparation. The inset in panel C reveals the fine structure of the exotherm seen in the descending scan of the hydrated preparation. Other conditions were as described in Figure 1.

and descending temperature modes at a scan rate of 10 °C/h (unless otherwise noted). After base-line subtraction and correction for the instrument thermal response, the calorimetric data were analyzed to yield phospholipid excess heat capacities as a function of temperature and enthalpy changes by employing software supplied by Hart. For a given transition, $T_m$ was taken to be the temperature of the maximal excess heat capacity, and $\Delta T_{1/2}$ was taken as the transition width at half-maximal excess heat capacity.

## Results

*DSC of Unhydrated Samples.* The endothermic transition profiles of unhydrated preparations of C(18)C(18)PE through C(18)C(10)PE are shown in panel A of Figures 1–5, respectively. The corresponding thermodynamic parameters are listed in Table I. The C(18)C(18)PE sample (Figure 1A) shows a single, asymmetric transition endotherm that is broadened on the low-temperature side of the transition. The calorimetrically determined $\Delta H$ (transition enthalpy) is 22.2 kcal/mol. This transition enthalpy is larger than that observed (12.9 kcal/mol) by Chowdhry et al. (1984). We consistently observed transition enthalpies between 20 and 25 kcal/mol for two lots of C(18)C(18)PE from Avanti Polar Lipids and for one lot from Sigma Chemical Co. The C(18)C(16)PE preparation (Figure 2A) exhibits an asymmetric transition endotherm with a partially resolved shoulder on the high-temperature side of the transition. The endothermic transition profile of unhydrated C(18)C(14)PE (Figure 3A) is very broad and appears to consist of three highly overlapped transition endotherms that are only partially resolved. The apparent $T_m$s of these three transitions range from 58 to 62 °C. The detailed shape of the endothermic profile, with regard to the number of apparent transition peaks and their degree of resolution, varied somewhat for different unhydrated preparations of C(18)C(14)PE. Unhydrated samples of C(18)C(12)PE (Figure 4A) and C(18)C(10)PE (Figure 5A) display single, asymmetric transitions that are broadened on the low-temperature sides of the transitions.

The transition temperatures of the unhydrated PE samples increase systematically with an increase in molecular weight. In contrast, the transition enthalpies are not related in a simple way to the molecular weight of the PEs. With the exception of the relatively high value for C(18)C(18)PE, the transition enthalpies of the mixed acyl PEs are similar in value; they range from 12.2 to 14.6 kcal/mol.

No corresponding exothermic transitions were observed when these samples were scanned down in temperature from

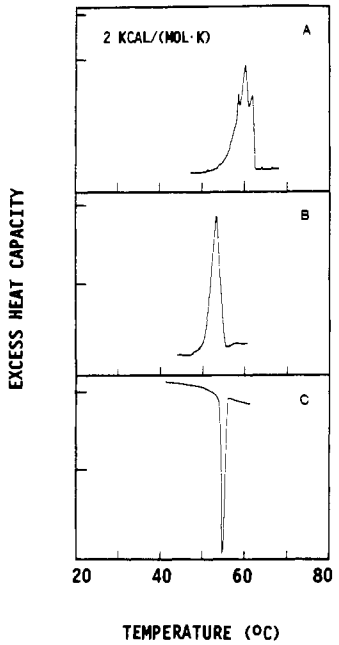


FIGURE 3: DSC profiles of C(18)C(14)PE in excess buffer. (A) Ascending scan of an unhydrated preparation. (B) Ascending scan of a hydrated preparation. (C) Descending scan of a hydrated preparation. Other conditions were as described in Figure 1.

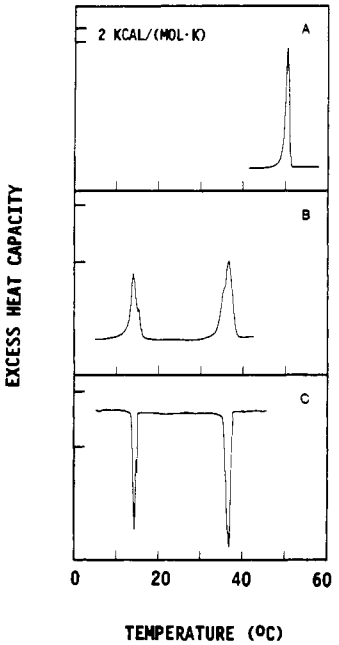


FIGURE 4: DSC profiles of C(18)C(12)PE in excess buffer. (A) Ascending scan of an unhydrated preparation. (B) Ascending scan of a hydrated preparation. (C) Descending scan of a hydrated preparation. The latter scan was conducted at 60 °C/h. Other conditions were as described in Figure 1.

temperatures above the endothermic transitions (data not shown). Thus, the endothermic transitions exhibited in ascending temperature scans of the unhydrated preparations are irreversible.

*$^{31}P$ NMR of Unhydrated Samples.* The low-temperature phases of the unhydrated PE samples were also investigated by $^{31}P$ NMR spectroscopy. Spectra consisting of up to 20000 scans failed to reveal any discernible $^{31}P$ NMR spectral features (data not shown). Thus, in the low-temperature phase of the PEs, the phosphate moiety is essentially immobilized on the $^{31}P$ NMR time scale. $^{31}P$ NMR spectra of the unhydrated PE preparations in their high-temperature phases

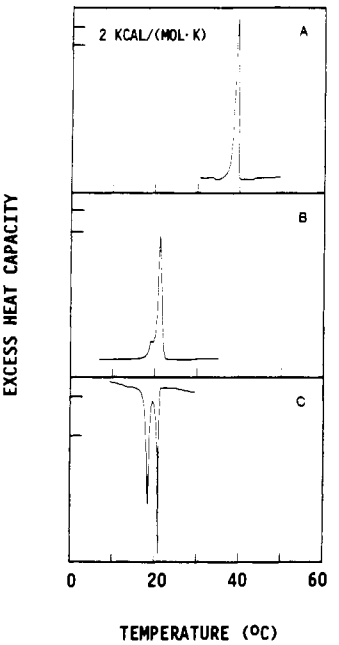


FIGURE 5: DSC profiles of C(18)C(10)PE in excess buffer. (A) Ascending scan of an unhydrated preparation. (B) Ascending scan of a hydrated preparation. (C) Descending scan of a hydrated preparation. Other conditions were as described in Figure 1.

revealed broad pseudoaxially symmetric powder patterns characterized by high-field peaks with broad low-field shoulders (data not shown). These spectral "bilayer" line shapes and their CSA values were identical with those obtained for the corresponding hydrated PE bilayers in their high-temperature phases. The characteristics of these $^{31}P$ NMR spectra will be described below.

*DSC of Hydrated Samples.* The transition profiles of hydrated samples of C(18)C(18)PE through C(18)C(10)PE are shown in panel B (ascending temperature scans) and panel C (descending temperature scans) of Figures 1–5, respectively. C(18)C(18)PE (Figure 1B), C(18)C(16)PE (Figure 2B), and C(18)C(14)PE (Figure 3B) all display single asymmetric gel to liquid-crystalline phase transitions that are broadened on the low-temperature side of the transition endotherms. The transition temperatures and enthalpies decrease systematically with decreasing molecular weight, whereas the transition breadth increases with increasing chain length asymmetry (Table I). When hydrated samples of C(18)C(18)PE (Figure 1C) or C(18)C(16)PE (Figure 2C) were scanned down in temperature, exothermic transition profiles were observed, which appear to represent a composite of two highly overlapped transitions that are only partially resolved. The apparent $T_m$s of these two transitions differ by about 1 °C in each case. For both PEs, the two apparent exotherms remain discernible for scan rates as low as 2 °C/h. Exothermic liquid-crystalline to gel transition profiles consisting of two partially resolved peaks have also been reported for certain symmetric acyl PEs (Chang & Epand, 1983; Wilkinson & Nagle, 1981). In contrast, a descending temperature scan of hydrated C(18)-C(14)PE (Figure 3C) reveals a single symmetric liquid-crystalline to gel transition. For all three PEs, there is no significant hysteresis in the transition enthalpies, and the hysteresis in the transition temperatures averages 1.3 °C (with the exothermic $T_m$s being lower in value) at scan rates of 10 °C/h.

The endothermic transition profile of C(18)C(12)PE (Figure 4B) consists of two asymmetric transitions, one at 13.9 °C and a second at 36.9 °C. The descending temperature transition

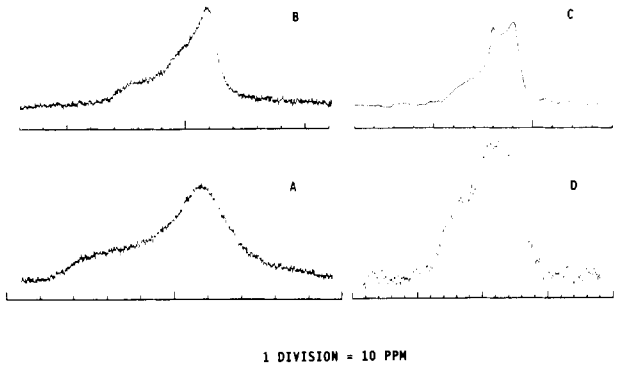


FIGURE 6: Representative proton-decoupled 24.1-MHz $^{31}P$ NMR spectra of the mixed acyl PEs in excess buffer. (A) Hydrated C(18)C(16)PE at 50 °C. (B) Hydrated C(18)C(16)PE at 70 °C. (C) Hydrated C(18)C(14)PE at 60 °C. (D) Hydrated C(18)C(10)PE at 5 °C. Phospholipid concentrations were 100 mg/mL. A 4000-Hz sweep width was employed, and 4000 data points were collected with 5000–10 000 scans accumulated per spectrum at a delay of 1 s between pulses.

profile of C(18)C(12)PE (Figure 4C and Table I) reveals two exotherms, one at 35.3 °C and a second at 12.4 °C. Clearly, the two exothermic transitions observed during the descending temperature scan of the hydrated C(18)C(12)PE bilayers indicate that the two corresponding endothermic phase transitions are reversible. Due to the metastable behavior of C(18)C(12)PE (discussed below), the descending scans were performed at a scan rate of 60 °C/h. The hysteresis in the transition temperatures averages 1.4 °C at this scan rate, and the transition enthalpies display no significant hysteresis.

Hydrated samples of C(18)C(10)PE (Figure 5B) reveal a single asymmetric endothermic transition. The descending temperature scan of C(18)C(10)PE (Figure 5C) reveals two partially overlapped exothermic transitions, one at 20.1 °C and a second at 17.9 °C. The C(18)C(10)PE exothermic transition profile does not change significantly for scan rates as low as 2 °C/h.

*$^{31}P$ NMR of Hydrated Samples.* The 24.15-MHz proton-decoupled $^{31}P$ NMR spectra of several of the hydrated mixed acyl PEs at various temperatures are shown in Figures 6 and 7. The low-temperature spectrum of hydrated C(18)C(16)PE at 50 °C is shown in Figure 6A. This broad pseudoaxially symmetric powder pattern is characterized by a high-field peak with a broad low-field shoulder. The CSA, determined from the separation between the intersection of tangents drawn to the points of maximum slope on the high- and low-field edges of the spectrum with the base line (Herzfield et al., 1978), is about 65 ppm. The low-temperature phases of C(18)C(18)PE and C(18)C(14)PE give essentially identical spectra (data not shown), with CSA values ranging from 65 to 69 ppm. The high-temperature spectrum of hydrated C(18)C(16)PE at 70 °C is shown in Figure 6B. Here, the bilayer line shape is characterized by a narrower CSA of about 49 ppm. A similar spectrum (CSA = 49 ppm) is obtained for the high-temperature phase of C(18)C(18)PE. The spectrum of hydrated C(18)C(14)PE at 60 °C is shown in Figure 6C. The spectrum represents the superposition of a liquid-crystalline bilayer pattern and a narrow emerging downfield resonance. The chemical shift of this partially resolved spectral component indicates that it does not represent an emerging isotropic phase or a hexagonal ($H_{II}$) phase (Cullis & de Kruijff, 1978). We have observed a similar spectrum for C(18)C(14)PC bilayers in the liquid-crystalline phase (unpublished experiments). It has been shown by negative-stain (Mason et al., 1983) and freeze–fracture (Hui et al., 1984) electron microscopy that the gel to liquid-crystalline transition of C(18)C(14)PC is

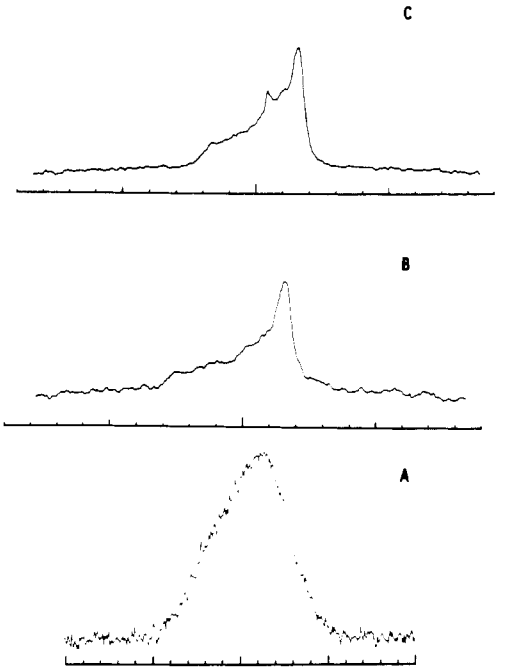


FIGURE 7: Proton-decoupled 24.1-MHz $^{31}P$ NMR spectra of hydrated C(18)C(12)PE in the three phases surrounding the two endothermic phase transitions. (A) Hydrated C(18)C(12)PE at 5 °C. (B) Hydrated C(18)C(12)PE at 25 °C. (C) Hydrated C(18)C(12)PE at 45 °C. Other conditions were as described in Figure 6.

accompanied by the spontaneous breakdown of some of the large multilamellar bilayers into smaller vesicles with diameters of approximately 1000 Å. This yields a morphologically heterogeneous population with a bimodal distribution of liposomal sizes. A similar phenomenon may occur in hydrated preparations of C(18)C(14)PE. The observed narrow line shape in the spectrum is caused primarily by the additional motional averaging of the lipid headgroups as a result of rapid lateral diffusion of the phospholipid molecules in the intermediate-sized vesicles (Burnell et al., 1980). The $^{31}P$ NMR spectrum of hydrated C(18)C(10)PE in the low-temperature phase at 5 °C is shown in Figure 6D. Although the bilayer line shape is largely evident, the spectrum is broadened, and the CSA is 82 ppm. The spectrum of C(18)C(10)PE at 30 °C (data not shown) is similar to that of C(18)C(16)PE in its high-temperature phase.

$^{31}P$ NMR spectra have been recorded for hydrated bilayers of C(18)C(12)PE in the three phases surrounding the two endothermic phase transitions. The spectrum in the low-temperature phase at 5 °C (Figure 7A) resembles the corresponding C(18)C(10)PE spectrum at the same temperature. A broadened bilayer line shape is observed with a CSA of about 82 ppm. The low-temperature phase transition produces a considerable narrowing of the spectrum along with a reduction of the CSA to 59 ppm. The spectrum for the PE in the middle-temperature phase at 25 °C is shown in Figure 7B. This spectrum strongly resembles the low-temperature spectrum of C(18)C(16)PE. The C(18)C(12)PE spectrum in the high-temperature phase at 45 °C (Figure 7C) is an axially symmetric powder pattern with a CSA of 47 ppm. This spectrum is distorted near the center by a narrow, emerging resonance line shape. This characteristic spectrum strongly resembles that of C(18)C(14)PE in the high-temperature phase. Finally, the $^{31}P$ NMR spectra of the unhydrated PE preparations in their high-temperature phases are identical

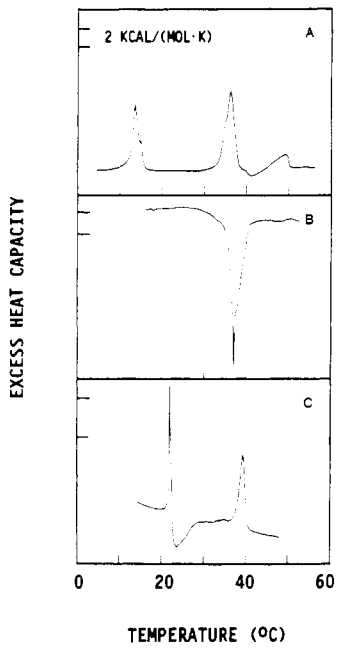


FIGURE 8: DSC profiles of C(18)C(12)PE and C(18)C(10)PE revealing the metastable behavior of these preparations. (A) Ascending scan of hydrated C(18)C(12)PE from 10 to 60 °C at 10 °C/h. (B) Descending scan of hydrated C(18)C(12)PE at a scan rate of 10 °C/h. (C) Ascending scan of a preparation of C(18)C(10)PE at 10 °C/h immediately after the initial scan of an unhydrated preparation. Other conditions were as described in Figure 1.

with those described above for the high-temperature phases of the corresponding hydrated PE samples.

*Metastable Behavior of the Mixed Acyl PEs.* Certain aspects of the metastable behavior of the mixed acyl PEs have been investigated. Dispersions of C(18)C(18)PE, C(18)C(16)PE, and C(18)C(14)PE exhibited no significant metastable behavior under the experimental conditions employed in this study. Ascending and descending temperature scans conducted subsequent to the initial ascending temperature scans of the unhydrated preparations were identical with scans conducted with well-hydrated samples. Fully hydrated samples of the above PEs were held at 0 °C for 2 weeks and then analyzed by DSC. This treatment resulted in no change in the thermotropic behavior of dispersions of C(18)C(18)PE or C(18)C(16)PE. For dispersions of C(18)C(14)PE, this incubation led to the regeneration of a small amount of the crystalline phase as evidenced by the appearance of an endothermic profile between 58 and 62 °C (data not shown).

The ascending temperature scan shown in Figure 4B for the hydrated C(18)C(12)PE sample was stopped immediately after the completion of the transition at 36.9 °C. An ascending temperature scan from 10 to 60 °C of a hydrated preparation of C(18)C(12)PE is shown in Figure 8A. Immediately after the completion of the transition at 36.9 °C, a broad exothermic transition is observed between 38 and 43 °C. This exotherm is immediately followed by a small endotherm with a $T_m$ of 48 °C. The transition enthalpies of the exotherm and endotherm are both about 4 kcal/mol. To examine the metastable behavior further, hydrated samples of C(18)C(12)PE were incubated for 24 h at 42 °C (in the high-temperature phase), 25 °C (in the middle-temperature phase), or 10 °C (in the low-temperature phase). These samples were then cooled to 5 °C and scanned to 60 °C (data not shown). The sample incubated at 5 °C yielded a transition profile identical with that shown in Figure 8A. However, the samples incubated at 25 or 42 °C produced a transition profile identical with the one obtained for the unhydrated preparation of C(18)C(12)PE (Figure 4A). The exothermic transition profile of the hydrated C(18)C(12)PE sample shown in Figure 4C was obtained at a descending scan rate of 60 °C/h. The exothermic transition profile of a hydrated C(18)C(12)PE sample scanned at −10 °C/h is shown in Figure 8B. A broad, asymmetric transition profile is observed, which appears to consist of two or thee highly overlapped transition exotherms that are only partially resolved. The transition enthalpy for the composite transition is about 12 kcal/mol. When this preparation was rescanned in the ascending temperature direction, a transition profile identical with that for the unhydrated preparation of C(18)C(12)PE (Figure 4A) was obtained.

For preparations of C(18)C(10)PE, the thermal behavior during descending temperature scans was independent of thermal history and always resembled the exothermic profile shown in Figure 5C. Repeated ascending temperature scans subsequent to the initial scan of an unhydrated preparation yielded the profile shown in Figure 8C. Here, the endothermic transition at 21.1 °C, typical of a hydrated preparation, is observed with the normal transition enthalpy (9.2 kcal/mol). Immediately after this transition, a broad exotherm is observed between 23 and 37 °C, with a transition enthalpy of about 12 kcal/mol. A second endotherm is then seen with a $T_m$ of 39.2 °C and a transition enthalpy of about 12 kcal/mol. The latter endotherm is identical with that observed for unhydrated preparations of C(18)C(10)PE (Figure 5A). In another experiment, a sample of hydrated C(18)C(10)PE was incubated at 25 °C for 24 h, cooled to 0 °C, and scanned to 50 °C. The resulting transition profile was identical with that shown in Figure 5A for the unhydrated preparation of C(18)C(10)PE (data not shown).

## Discussion

We have been studying the effects of asymmetry in the length of the two constituent acyl chains on the bilayer properties of saturated mixed acyl phospholipids. The bilayer properties of these PCs have been discussed in detail in previous publications (Mason et al., 1981b; Huang et al., 1983; Hui et al., 1984), including a recent review article (Huang & Mason, 1986). An understanding of the packing properties of the mixed acyl phospholipids has been facilitated by a thermodynamic analysis of their phase transitions. The normalized transition entropy ($\Delta S/\Delta S_{exp}$) of these transitions is plotted against the magnitude of the chain inequivalance ($\Delta C/CL$) of the mixed acyl phospholipids, where $\Delta C$ is the absolute difference in the length of the two fatty acyl chains and $CL$ is the length of the longer of the two fatty acyl chains. A detailed discussion of this thermodynamic analysis has been given elsewhere (Mason et al., 1981b; Huang & Mason, 1986). This analysis has been applied to the unhydrated and hydrated transitions exhibited by the mixed acyl PEs. The corresponding plot is shown in Figure 9.

*Unhydrated Samples.* The endothermic phase transitions exhibited during the initial ascending temperature scans of the unhydrated PE preparations are assigned to be crystalline to liquid-crystalline phase transitions. These transitions correspond to the simultaneous hydration and acyl chain melting of poorly hydrated crystalline samples. Several lines of evidence support this assignment. The $^{31}P$ NMR spectra of the unhydrated PEs in their low-temperature phases failed to reveal any discernible spectral features, even for spectra consisting of up to 20000 scans. The $^{31}P$ NMR spectra of C(16)C(16)PC in the bilayer crystalline subphase are characterized by a partially averaged, axially asymmetric powder pattern with a CSA of about 180 ppm at 109 MHz (Füldner,

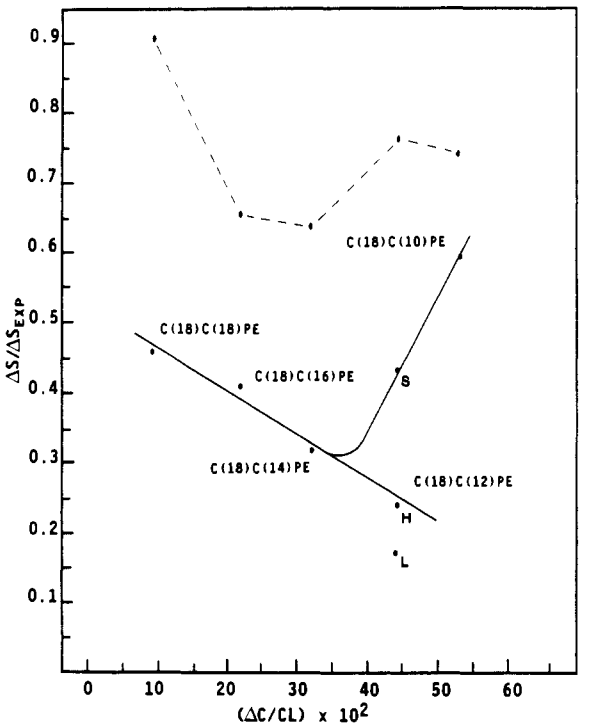


FIGURE 9: Plot of the normalized transition entropy as a function of the chain inequivalence parameter for the mixed acyl PEs. These parameters were calculated as described in the text. Transitions for both the unhydrated preparations (---) and the hydrated samples (—) are shown. For hydrated samples of C(18)C(12)PE, values are indicated for the low-temperature transition (L), the high-temperature transition (H), and the sum of these two transitions (S).

1981). Therefore, the phosphate moiety of the PE headgroups must undergo a slower rate of axial diffusion than is the case for C(16)C(16)PC in the crystalline subphase. In contrast, the $^{31}P$ NMR spectra of the unhydrated PE preparations in their high-temperature phases are broad pseudoaxially symmetric powder patterns characterized by high-field peaks and broad low-field shoulders with CSA values between 47 and 49 ppm. This spectral bilayer line shape can be quantitatively explained by a model for phospholipid dynamics that assumes rapid ($>10^4$ $s^{-1}$) rotation of the phospholipid molecule, as a whole, around the bilayer normal (Herzfield et al., 1978; Campbell et al., 1979) coupled with fast rotation about the $C_2$–$C_3$ glycerol bond that occurs in the liquid-crystalline bilayer phase (Gally et al., 1981). Thus, the temperature-dependent $^{31}P$ NMR results for the unhydrated PE preparations are consistent with a transition from a highly ordered crystalline phase to the liquid-crystalline bilayer phase.

The thermodynamics of these endothermic phase transitions also support this conclusion. The transition endotherms of the unhydrated preparations occur at a higher temperature ($T_{m+h}$) and with a larger transition enthalpy than the endothermic transitions of the corresponding hydrated samples. These latter phase transitions are shown below to correspond to gel to liquid-crystalline bilayer transitions. By analogy with saturated symmetric chain PEs (Chang & Epand, 1983; Mantsch et al., 1983; Chowdhry et al., 1984), this higher melting, larger enthalpy transition is ascribed to the melting of a highly ordered, poorly hydrated crystalline phase that is stable over its entire temperature range until it melts to the liquid-crystalline phase at $T_{m+h}$.

A plot of the normalized transition entropies of the unhydrated PEs as a function of their chain length asymmetries is shown in Figure 9. The normalized transition entropy decreases from C(18)C(18)PE to C(18)C(14)PE and then increases slightly for C(18)C(12)PE and C(18)C(10)PE. This can be taken to indicate that the exact crystalline polymorph, and possibly the degree of headgroup hydration, is critically dependent upon the length of both acyl chains. The endothermic transition profile of unhydrated C(18)C(14)PE consists of several highly overlapped transition endotherms that were only partially resolved. In general, different crystalline polymorphs of the PEs are obtained depending upon the conditions and solvents employed for recrystallization. For example, C(12)C(12)PE recrystallized from chloroform yields type II crystals that are less ordered than the type I crystals obtained from ethanol. The former crystals display overlapped transition endotherms when scanned as unhydrated preparations (Mantsch et al., 1983). It appears that the splitting of the transition profile seen in unhydrated samples is most likely correlated with PE crystalline polymorphs of heterogeneous structure.

*Hydrated Samples.* Hydrated samples of C(18)C(18)PE, C(18)C(16)PE, and C(18)C(14)PE exhibit $^{31}P$ NMR spectra with bilayer line shapes and CSA values of 62–69 ppm when analyzed at temperatures below their respective $T_m$s immediately after cooling from 80 °C. At temperatures above their respective $T_m$s, these three PEs exhibit bilayer line shapes with CSA values of 47–49 ppm. Thus, the endothermic transitions of hydrated samples of C(18)C(18)PE, C(18)C(16)PE, and C(18)C(14)PE are assigned as being gel to liquid-crystalline phase transitions (Gally et al., 1981; Brown & Seelig, 1978). As shown in Figure 9, the normalized transition entropies for these three PEs decrease in a linear correlation with an increase in $\Delta C/CL$. This same trend has been observed for the corresponding mixed chain PCs (Mason et al., 1981b). In fact, the points for the mixed acyl PCs and PEs are virtually superimposable. This trend is interpreted to indicate that the gel phase hydrocarbon chains pack without significant interdigitation of the acyl chains across the bilayer center. X-ray diffraction studies have shown that this is the predominant mode of gel phase packing for the phospholipids in this region (Hui et al., 1984).

Descending temperature scans of hydrated C(18)C(18)PE and C(18)C(16)PE revealed exothermic transition profiles that appeared to consist of two highly overlapped transitions that were only partially resolved. We currently have no explanation for this phenomenon or why it is revealed only during descending temperature scans. However, this splitting is also observed in descending temperature scans of hydrated samples of saturated symmetric acyl PEs [C(12)C(12)PE, C(14)C(14)PE, C(16)C(16)PE, and C(18)C(18)PE, unpublished experiments]. In addition, the relative proportions of the two peaks (the apparent transition enthalpy of the higher temperature transition vs the lower temperature transition) are sensitive to the thermal history of the sample and the protocol employed to hydrate the lipid. This result suggests that the peak splitting may have its origins in processes related to the hydration-dependent inter- and intralamellar organization of the PE polar headgroup region. Alternately, the two transitions could arise from a decoupling of the chain melting and dehydration processes during cooling of the sample, resulting in the formation of a metastable intermediate. In either case, the persistence of the two apparent exotherms at a scan rate of 0.033 °C/min is indicative of a slow process or a long-lived intermediate. The process responsible for the two-peak transition exotherm is clearly sensitive to the hydrocarbon chain composition of the PE as C(18)C(14)PE displays a single sharp exotherm. We are continuing to investigate this phenomenon and will report our findings in a future publication.

Hydrated bilayers of C(18)C(12)PE exhibit two endothermic transitions when scanned immediately subsequent to cooling from 80 °C. The normalized transition entropy for the high-temperature transition at 36.9 °C (point H in Figure 9) is found to conform to the same linear trend defined by C(18)C(18)PE, C(18)C(16)PE, and C(18)C(14)PE. This strongly suggests that the high-temperature transition of C(18)C(12)PE is a noninterdigitated gel to liquid-crystalline phase transition. The $^{31}$P NMR spectra observed for this PE below (CSA = 59 ppm) and above (CSA = 47 ppm) the 36.9 °C transition support this assignment. The $^{31}$P NMR spectra of C(18)C(12)PE at a temperature (5 °C) below the low-temperature transition at 13.9 °C reveal a bilayer line shape, but it is broadened and has a CSA of 82 ppm. This large value for the CSA suggests that the C(18)C(12)PE bilayer is packed in a mixed-interdigitated conformation at temperatures below the low-temperature transition. In this packing conformation, the short chains pack end-to-end, and the long stearoyl chains span the entire hydrocarbon width of the bilayer (Huang & Mason, 1986). In noninterdigitated bilayers, each phospholipid molecule is free to rotate independently. However, in mixed-interdigitated bilayers, the conformational coupling of the phospholipid molecules across the bilayer requires that the fundamental packing unit be a dimer. This dimeric unit will undergo axial rotation at a slower rate than will the monomeric unit in noninterdigitated bilayers. The larger CSA observed for mixed-interdigitated bilayers is a consequence of this reduced rotational motion (Xu et al., 1987). Thus, the low-temperature transition of C(18)C(12)PE is assigned to be a mixed-interdigitated to noninterdigitated gel transition. This assignment is further supported by the observation that the sum of the normalized transition entropies for the two transitions of C(18)C(12)PE (point S in Figure 9) is virtually identical with the value for C(18)C(12)PC (Mason et al., 1981b). Bilayers of C(18)C(12)PC undergo a single mixed-interdigitated gel to liquid-crystalline transition. The two phase transitions of C(18)C(12)PE are reversible upon fast cooling.

The $^{31}$P NMR spectrum for hydrated C(18)C(10)PE samples at 5 °C exhibits a broadened bilayer line shape with a CSA of 82 ppm, whereas in the high-temperature phase a narrower bilayer line shape with a CSA of 47 ppm is observed. In addition, the normalized transition entropy for C(18)C(10)PE is virtually identical with the value for bilayers of C(18)C(10)PC (Mason et al., 1981b). Thus, the single transition of hydrated C(18)C(10)PE is assigned to be a mixed-interdigitated gel to liquid-crystalline phase transition, analogous to the single transition of C(18)C(10)PC (Hui et al., 1984).

It is noteworthy that the thermodynamic parameters obtained for C(18)C(10)PE ($T_m$ = 21.1 °C, $\Delta H$ = 9.2 kcal/mol) are very similar to those obtained for C(18)C(10)PC ($T_m$ = 19.1 °C, $\Delta H$ = 9.9 kcal/mol). The higher transition temperatures of PE dispersions relative to their PC counterparts have been attributed primarily to the strong hydrogen-bonding interactions between the PE headgroups, which are absent in the PCs (Mabrey & Sturtevant, 1978; Boggs, 1980). In the mixed-interdigitated bilayer, each phospholipid headgroup must span three acyl chains, which leads to an expanded headgroup area relative to the noninterdigitated bilayer. This greater headgroup area would be predicted to result in a significant weakening, or elimination, of the hydrogen-bonding interactions between the PE headgroups. The similarity in the thermodynamic parameters for the mixed-interdigitated gel to liquid-crystalline transitions of the C(18)C(10)PE and C(18)C(10)PC bilayers is in accordance with this prediction.

Results obtained with the mixed acyl PEs are analogous to those obtained with certain cerebroside sulfates (Boggs et al., 1988). On the basis of DSC and electron spin resonance spectroscopic data, *N*-lignoceroylcerebroside sulfate (C24:0-CBS) undergoes two endothermic transitions upon heating. The first is the transition of a mixed-interdigitated gel phase to a partially interdigitated gel phase, whereas the second is that of a partially interdigitated gel phase to a liquid-crystalline phase. These two transitions are reversible upon cooling. The behavior of C24:0-CBS is clearly analogous to that of C(18)C(12)PE. This pattern of thermotropic behavior is also exhibited by hydrated dispersions of DL-*erythro*-*N*-lignoceroylsphingophosphocholine (Levin et al., 1985). Aqueous suspensions of *N*-certoylcerebroside sulfate (C26:0-CBS) exhibit a single mixed-interdigitated gel to liquid-crystalline phase transition analogous to C(18)C(10)PE. Upon cooling, the C26:0-CBS liquid-crystalline phase transforms to the mixed-interdigitated phase in a three-stage process. These three stages were assigned to be the reformation of the trans chains, the transformation to the partially interdigitated gel phase, and finally the formation of the mixed-interdigitated gel phase (Boggs et al., 1988). On the basis of these findings, the two partially resolved exotherms seen during the descending temperature scans of the hydrated C(18)C(10)PE dispersions are proposed to be the liquid-crystalline to partially interdigitated gel transition followed by the transition of the latter phase to the mixed-interdigitated gel phase.

The current study as well as others (Boggs et al., 1988; Levin et al., 1985; Xu & Huang, 1987) has demonstrated that phospholipids and glycosphingolipids with $\Delta C/CL$ values close to 0.5 can most efficiently compensate for the disordering effects of chain length asymmetry by adopting a mixed-interdigitated packing. However, the adoption of this gel phase packing comes at the expense of reducing, or eliminating, energetically favorable polar headgroup interactions, when present. The partially interdigitated gel phase packing preserves these polar headgroup interactions, but at the expense of a more disordered chain packing. Thus, which of these two gel phase packings are adopted by one of the aforementioned lipids at a given temperature depends critically upon the energetic balance of the interactions occurring within these two regions of the lipid molecule.

*Metastability of the Mixed Acyl PEs.* Dispersions of C(18)C(18)PE, C(18)C(16)PE, and C(18)C(14)PE exhibited no significant metastable behavior under the experimental conditions employed in this study. In contrast, preparations of C(18)C(10)PE and C(18)C(12)PE exhibited pronounced metastable behavior. The thermotropic behavior of C(18)C(10)PE can be interpreted to indicate that the liquid-crystalline phase in the temperature interval between $T_m$ and $T_{m+h}$ ($\Delta T$ region) is metastable with respect to the crystalline phase. This metastability is enhanced in samples where the polar headgroups of the PEs are not fully hydrated due to the incomplete equilibration of water throughout the dispersions. The temperature dependence and the scan rate dependence of the metastable liquid-crystalline to crystalline transition suggest that this conversion proceeds by a nucleation and growth process. Nucleation occurs at a significant rate only at temperatures near $T_m$. However, once stable nuclei have formed, complete conversion to the crystalline phase will proceed at higher temperatures within the $\Delta T$ region.

Thus, when fully hydrated samples of C(18)C(10)PE are scanned up in temperature at rates of 10 °C/h or higher, no metastable behavior is observed since the scan rate is too fast to allow for nucleation to occur. However, if these samples

are incubated at temperatures between 23 and 28 °C for 24 h, complete conversion to the crystalline phase is observed. When incompletely hydrated samples of C(18)C(10)PE are scanned up in temperature at a rate of 60 °C/h, no metastable behavior is observed. However, at a scan rate of 10 °C/h, nucleation can occur at temperatures just above $T_m$, and the entire metastable liquid-crystalline phase transforms exothermically to the crystalline phase between 23 and 37 °C. The crystalline to liquid-crystalline transition is then observed at 39 °C. When fully hydrated preparations of C(18)C(10)PE are held at 0 °C, a complex metastable behavior is observed. A study of this metastability will be reported in a future publication.

Fully hydrated dispersions of C(18)C(12)PE also exhibited metastable behavior of the liquid-crystalline phase within the $\Delta T$ region. Even at ascending scan rates as high as 60 °C/h, an exothermic transition of the liquid-crystalline phase to a stable intermediate was observed between 38 and 43 °C. This stable intermediate melts to the liquid-crystalline phase at 48 °C and may be analogous to the $\beta_1$ phase formed by hydrated dispersions of C(12)C(12)PE (Seddon et al., 1983). The metastability of the liquid-crystalline phase is also manifested during descending temperature scans. At a descending scan rate of 10 °C/h, the metastable liquid-crystalline phase undergoes a direct exothermic conversion to the crystalline phase in a three-stage (or more) process. Incubation of hydrated samples of C(18)C(12)PE in the liquid-crystalline phase at 42 °C or in the noninterdigitated gel phase at 25 °C for 24 h also results in the conversion to the crystalline phase. In contrast, prolonged incubation of the mixed-interdigitated gel phase at 0 °C did not result in the regeneration of the crystalline phase. This is similar to the behavior of hydrated bilayers of C24:0-CBS, where it was shown that the liquid-crystalline and partially interdigitated gel phases, but not the mixed-interdigitated gel phase, were capable of transforming to more ordered, less hydrated phases (Boggs et al., 1988). Ascending temperature scans performed immediately subsequent to the initial scan of an unhydrated preparation of C(18)C(12)PE would frequently reveal the exothermic conversion of the noninterdigitated gel phase to the crystalline phase at temperatures between 14 and 35 °C (data not shown). These preparations failed to reveal the noninterdigitated gel to liquid-crystalline transition. Thus, the conversion of the metastable noninterdigitated gel phase to the crystalline phase appears to be enhanced in C(18)C(12)PE bilayers that have not been completely hydrated.

## References


Boggs, J. M. (1980) *Can. J. Biochem. 58*, 755.

Boggs, J. M., Koshy, K., & Rangaraj, G. (1988) *Biochim. Biophys. Acta 938*, 373.

Brown, M. F., & Seelig, J. (1978) *Biochemistry 17*, 381.

Burnell, E. E., Cullis, P. R., & de Kruijff, B. (1980) *Biochim. Biophys. Acta 603*, 63.

Campbell, R. F., Meirovitch, E., & Freed, J. H. (1979) *J. Phys. Chem. 83*, 527.

Chang, H., & Epand, R. M. (1983) *Biochim. Biophys. Acta 728*, 319.

Chowdhry, B. Z., Lipka, G., Dalziel, A. W., & Sturtevant, J. M. (1984) *Biophys. J. 45*, 901.

Comfurius, P., & Zwaal, R. F. A. (1977) *Biochim. Biophys. Acta 488*, 36.

Cullis, P. R., & de Kruijff, B. (1978) *Biochim. Biophys. Acta 507*, 207.

Füldner, H. H. (1981) *Biochemistry 20*, 5707.

Gally, H. U., Pluschke, G., Overath, P., & Seelig, J. (1981) *Biochemistry 20*, 1826.

Herzfield, J., Griffin, R. G., & Haberkorn, R. H. (1978) *Biochemistry 17*, 2711.

Huang, C., & Mason, J. T. (1986) *Biochim. Biophys. Acta 864*, 423.

Huang, C., Mason, J. T., & Levin, I. W. (1983) *Biochemistry 22*, 2775.

Huang, C., Mason, J. T., Stephenson, F. A., & Levin, I. W. (1986) *Biophys. J. 49*, 587.

Hui, S. W., Mason, J. T., & Huang, C. (1984) *Biochemistry 23*, 5570.

Levin, I. W., Thompson, T. E., Barenholz, Y., & Huang, C. (1985) *Biochemistry 24*, 6282.

Mabrey, S., & Sturtevant, J. M. (1978) *Methods Membr. Biol. 9*, 237.

Mantsch, H. H., Hsi, S. C., Butler, K. W., & Cameron, D. G. (1983) *Biochim. Biophys. Acta 728*, 325.

Mason, J. T., Broccoli, A. V., & Huang, C. (1981a) *Anal. Biochem. 113*, 96.

Mason, J. T., Huang, C., & Biltonen, R. L. (1981b) *Biochemistry 20*, 6086.

Mason, J. T., Huang, C., & Biltonen, R. L. (1983) *Biochemistry 22*, 1013.

Mulukutla, S., & Shipley, G. G. (1984) *Biochemistry 23*, 2514.

Overath, P., & Thilo, L. (1978) *Int. Rev. Biochem. 19*, 1.

Rouser, G., Nelson, G. J., Fleischer, S., & Simon, G. (1986) in *Biological Membranes* (Chapman, D., Ed.) p 5, Academic Press, New York.

Seddon, J. M., Harlos, K., & Marsh, D. (1983) *J. Biol. Chem. 258*, 3850.

Seddon, J. M., Cevc, G., Kaye, R. D., & Marsh, D. (1984) *Biochemistry 23*, 2634.

Wilkinson, D. A., & Nagle, J. F. (1981) *Biochemistry 20*, 187.

Wilkinson, D. A., & Nagle, J. F. (1984) *Biochemistry 23*, 1538.

Xu, H., & Huang, C. (1987) *Biochemistry 26*, 1036.

Xu, H., Stephenson, F. A., & Huang, C. (1987) *Biochemistry 26*, 5448.

Xu, H., Stephenson, F. A., Lin, H., & Huang, C. (1988) *Biochim. Biophys. Acta 943*, 63.